Biointerface Research in Applied Chemistry
Open-Access Journal (ISSN: 2069-5837)

Review
Volume 13, Issue 1, 2023, 79
https://doi.org/10.33263/BRIAC131.079

Mycobacterium tuberculosis Dihydrofolate Reductase Inhibitors: State of Art Past 20 Years

Sandra Valeria Vassiliades [1,†], Vitor Bastos Navarausckas [1,†], Marcio Vinícius Bertacine Dias [2], Roberto Parise-Filho [1,*]

[1] Department of Pharmacy, Faculty of Pharmaceutical Sciences, University of São Paulo, São Paulo, SP, Brazil
[2] Department of Microbiology, Institute of Biomedical Sciences, University of São Paulo, São Paulo, SP, Brazil
* Correspondence: roberto.parise@usp.br (R.P.F.);
† These authors contributed equally to this work;

Scopus Author ID 6507432437
Received: 3.12.2021; Accepted: 30.12.2021; Published: 6.02.2022

Abstract: Tuberculosis is a disease with a high level of incidence and mortality. Due to the problems associated with current therapy, it is necessary and urgent to develop new drugs for treatment. Dihydrofolate reductase (DHFR) is a recognized target for the action of several drugs. The 3D structure of the *Mycobacterium tuberculosis* DHFR (*Mt*DHFR) elucidates the key amino acid residues responsible for the active site architecture formation and structural basis for ligand specificity compared to the human DHFR (*h*DHFR). This article aims to offer a view on state of the art about new *Mt*DHFR inhibitors developed in the last twenty years. This study demonstrates a correlation between efficacy and the presence of specific groups, such as the diaminopyridimidine ring that binds to the enzyme active site and the similarity of the structures with classic DHFR inhibitors methotrexate. Herein, it is also reported the recent efforts to develop molecules non-traditional cores, which could be more selective and effective against tuberculosis.

Keywords: anti-tuberculosis; antimicrobial; *Mt*DHFR inhibitors; diaminopyridimidine; molecular docking; drug design; antifolates; glycerol pocket (GOL).

1. Introduction

1.1. Tuberculosis.

Tuberculosis (TB) is an infectious disease caused predominantly by *Mycobacterium tuberculosis* (*Mtb*) [1–3]. TB development depends on factors such as the patient's age and immunity and the latency period of the infection (common in 90% of cases) [4–6]. According to the World Health Organization (WHO)[7], 10 million new cases of TB emerge annually, and 1.5 million cases evolve to death, representing 14% of the cases reported in 2019. South-East Asia (44%) and Africa (25%) are the most affected countries. Drug-resistant TB was reported in 3.3% of the new cases and 17.7% of previously treated cases [7–13].

The mortality caused by TB can be significantly reduced by constant monitoring of cases and with the correct management of anti-TB therapy and regime [14–18]. However, anti-TB therapies have a prolonged treatment period and include several adverse effects that cause abandonment, which contributes to multidrug-resistant mycobacterial strain selection [19–25]. The difficulty in adhering to therapy, the increasing transmission of the etiological agent, and the arising of multidrug-resistant and extensively drug-resistant TB cases are factors that justify

the interest in the search for new strategies to control this disease, including the development of new anti-TB drugs [26–30].

1.2. Mycobacterium tuberculosis dihydrofolate reductase (MtDHFR).

The development of innovative molecules and drug candidates based on *Mtb* genomics and proteomics is a topic of intense research worldwide [22,29,31–35]. In this context, among other biological targets, *M. tuberculosis* dihydrofolate reductase (*Mt*DHFR), an NADPH-dependent key enzyme in the folate metabolism, is essential for mycobacterial growth [36,37].

*Mt*DHFR catalyzes the reduction of a double bond of dihydrofolic acid (DHF), mediated by hydride transfer, converting it into tetrahydrofolic acid (THF), which is an intermediate of other vital metabolic pathways for cell maintenance (Figure 1). Due to its critical role in regulating cellular THF, DHFR is a well-preserved regulatory enzyme in both eukaryotic and prokaryotic cells [38–41].

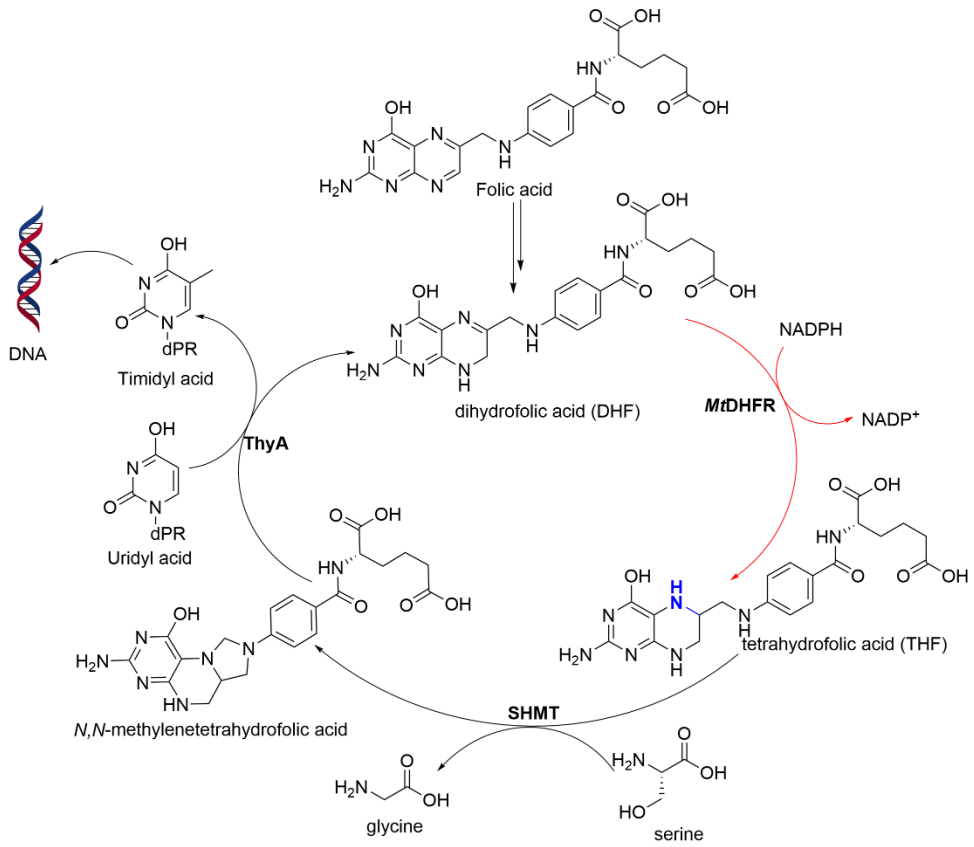

Figure 1. Simplified scheme of the metabolic pathway of folic acid. Enzymes in bold: *Mt*DHFR: *Mycobacterium tuberculosis* Dihydrofolate Reductase; SHMT: serine hydroxymethyltransferase; ThyA, thymidylate synthase (adapted from ref. 40 and 41).

In structural terms, *Mt*DHFR contains 159 amino acid residues, and its secondary structure is formed by a central β-sheet flanked by four α-helices. This β-sheet is formed by seven parallel strands and a C-terminal antiparallel strand (Figure 2A) [42,43]. *Mt*DHFR has 26% similarity to the amino acid sequence of *h*DHFR, and crystallographic studies of the two enzymes also demonstrated a similarity between overall protein folds [42,44,45].

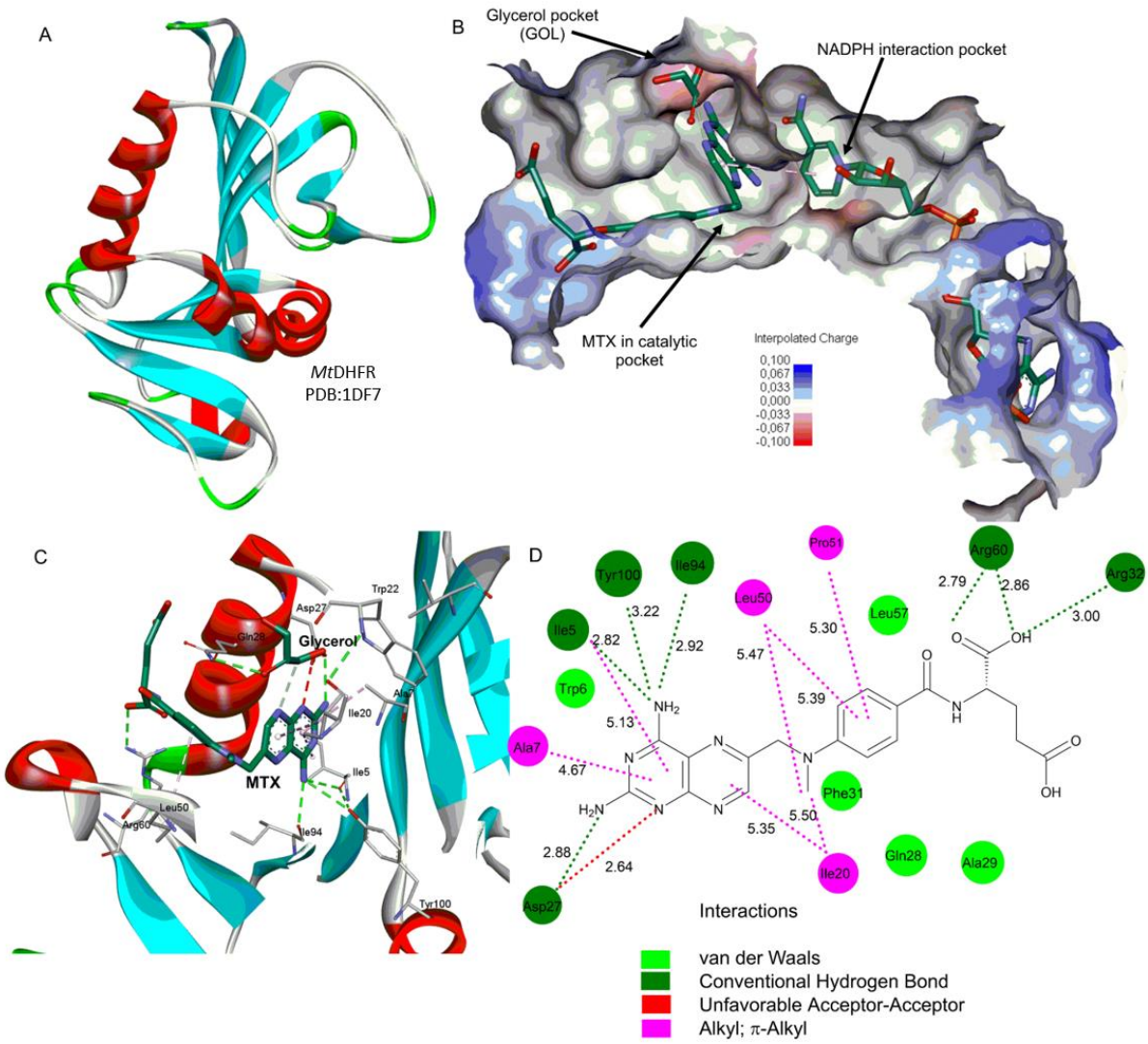

Figure 2. A) *Mt*DHFR structure (PDB: 1DF7). B) *Mt*DHFR catalytic site emphasizing the pteridinic moiety of MTX and the view of GOL and NADPH pocket. C) Interactions between residues of *Mt*DHFR active site (cartoon representation) with MTX and a glycerol molecule. D) 2D interactions between *Mt*DHFR and MTX. Distances in the color green indicate H-bonds. Distances in light pink indicate hydrophobic interactions. Images were drawn in Discovery Studio, Biovia.

In 2000, Li *et al*. [43] used antifolate methotrexate (MTX) and trimethoprim (TMP) as a ligand to study the interactions between the enzyme:ligand complex (Figure 2B-D). It was observed that MTX fits completely into the enzyme's catalytic pocket, and the 2,4-aminopterin ring interacts by hydrogen bonding with residues Ile5, Asp27, Ile94, and Tyr100 in addition to establishing a hydrophobic interaction with the NADPH molecule. The same interaction pattern was observed in the TMP:enzyme complex. Besides the hydrogen bonding interactions, MTX has many van der Waals contacts with the protein. For the side facing NADPH, the aminopterin interacts with Trp6, Ala7, and Ile20. The other side of the aminopterin ring interacts with Phe31, Ile5, Ile94, and Gln28 [43].

The *p*-aminobenzoyl ring of MTX interacts with five residues (Gln28, Phe31, Ile50, Pro51 and Leu57), creating a hydrophobic environment. The carboxylic acid of glutamate interacts freely with Arg32 and Arg60 residues by strong salt bridge and hydrogen bond interactions; these residues are often related to the enzyme's catalytic site [43].

Interestingly, in the same work, Li *et al*. [43] reported a small hydrophilic pocket in the structure of *Mt*DHFR near the diaminopterin binding site. A glycerol (GOL) molecule (crystallographic artifact) was observed to bind in this pocket interacting simultaneously with

MTX and residues Trp22, Asp27 and Gln28, forming an exclusive and extra binding pocket in *Mt*DHFR [42,45–48], which does not exist in human isoform (Figure 2B and 2C).[43] Consequently, this pocket has been used in structure-based drug discovery strategies to obtain selective compounds against *Mt*DHFR [46,49].

2. *Mt*DHFR Inhibitors (*Mt*DHFRi)

The search for new drugs against tuberculosis has been greatly reinforced with the association of advanced *in silico* techniques and information obtained from the three-dimensional structures of human and mycobacterial DHFR. Since the publication of the findings by Li *et al.* [43], a series of works aimed at the development of new *Mt*DHFR inhibitors have been published. As antifolate compounds are already well established in cancer research, these structures were the first to be explored. Next, we will highlight the main articles found in the literature over the last two decades.

2.1. Compounds with bioisosteric pteridine groups.

From the 6-substituted pteridine core, Cunha, Ramalho, and Reynolds [50] synthesized 18 derivatives with alkyl substituents on the phenolic ring in trans *ortho-meta* position (Figure 3), the compounds were evaluated for their antimycobacterial activity against H37Ra strain and enzyme inhibition activity for *Mt*DHFR and *h*DHFR.

All prepared compounds have anti-TB and inhibitory activity due to the presence of the pteridine ring. Among the most active compounds, the IC_{50} for *Mt*DHFR was 9.0 nM for 1, while 2-3 had an IC_{50} of 23 nM, while for *h*DHFR, the observed IC_{50} was 25 nM, 95 nM, and 1500 nM, for compounds 1-3, respectively.

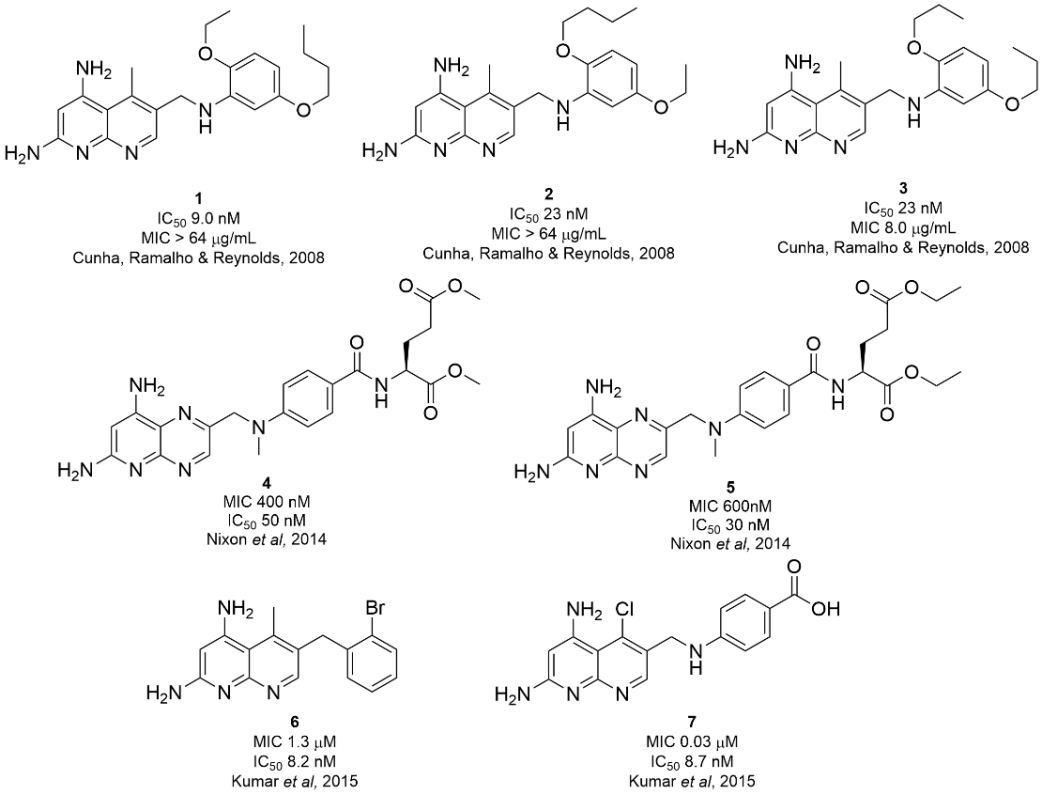

Figure 3. Chemical structure of a compound with bioisosteric pteridine core.

The maximum selectivity was observed for compound 3, substituted with a propyl group at the *ortho-meta* position of the phenolic ring. Interestingly, size modification

(increasing, decreasing the chain, or adding a heteroatom) lead to a loss of selectivity (1-2) [50].

In molecular docking studies, the authors observed that the cavity of the catalytic site of *Mt*DHFR is larger than that of *h*DHFR. Therefore smaller alkyl substituents can position themselves favorably in both enzymes, indicating that the selectivity of compound 3 may be related to the steric hindrance at the human DHFR binding site [50].

In 2014, Nixon *et al.* [51] synthesized and evaluated the inhibitory activity for *Mt*DHFR of MTX esters. Among the tested compounds, 4 and 5 (Figure 3) showed good activity against Mtb H_{37}Rv strain, with MIC values of 400 nM (4) and 600 nM (5), whereas in the enzyme inhibition assay, compound 5 was more active with an IC_{50} of 30 nM, while compound 5 had an IC_{50} of 50 nM.

For the authors, dialkyl esters increase the lipophilicity of the molecules, allowing better penetration through the mycobacterial cell wall. In tests executed with monoalkyl esters, although the inhibitory enzyme activity was not altered, there was a decrease in the anti-TB activity of these compounds, which are less lipophilic compared to 4-5 [51].

By a high-throughput screening of antifolate library belonging to the pharmaceutical GlaxoSmithKline (GSK), Kumar *et al.* [52] identified 17 structures derivatives from the pteridine ring as potential inhibitors for *Mt*DHFR. All selected compounds were tested against *Mtb* H_{37}Rv strain, and enzyme inhibition assay was performed in *Mtb* and human DHFR.

Although all compounds showed anti-TB activity, only 7 also showed inhibitory activity against *Mt*DHFR, especially compound 6 with a MIC of 1.3 μM and IC_{50} of 8.2 nM, and compound 7 with a MIC of 0.03 μM and IC_{50} of 8.7 nM, however, the compounds showed low selectivity for *Mt*DHFR. According to the authors, the good results observed for 7 would be related to its structural similarity with non-classical antifolates. The carboxylic acid group is a crucial factor for its activity [52].

2.2. Compounds with diamino heterocyclic rings.

In 2007, El-Hamamsy *et al*. designed and synthesized a series of 2,4-diaminopyrimidine C-substituted with trihydroxypentyl or trihydroxypropyl, aiming to explore the *Mt*DHFR GOL binding pocket. From 17 derivatives that were prepared, compound 8 (Figure 4), with a trihydroxypentyl side-chain, exhibited promising results in a qualitative biological assay against *M. tuberculosis* colonies [53].

Although there is no data on enzyme inhibition, through modeling studies of 8 with the human and *Mtb* DHFR, El-Hamamsy *et al.* reported that triol -chain acts as a GOL-mimicking group, occupying the same position and making the same hydrogen bond interaction as GOL in the crystal structure. Since the GOL binding pocket does not exist in *h*DHFR, the inhibitory activity in 8 indicated that the exploitation of this characteristic could provide more selectivity compounds [53].

Inspired by the structure proposed by El-Hamamsy *et al*., Degani's group evaluated the inhibitory activity for *Mt*DHFR and anti-TB against the H_{37}Rv *Mtb* strain from a series of diamino triazine ring derivatives. In the group's first work published in 2014 [54], 8 derivatives were synthesized. Still, only compound 9 (Figure 4) showed satisfactory results in the whole cell assay against H_{37}Rv strain with MIC of 8.9 μg/mL, thus being the only compound tested in an enzyme inhibition assay against *Mtb* and human DHFR showing an IC_{50} of 0.63 mM and 1.58 mM respectively.

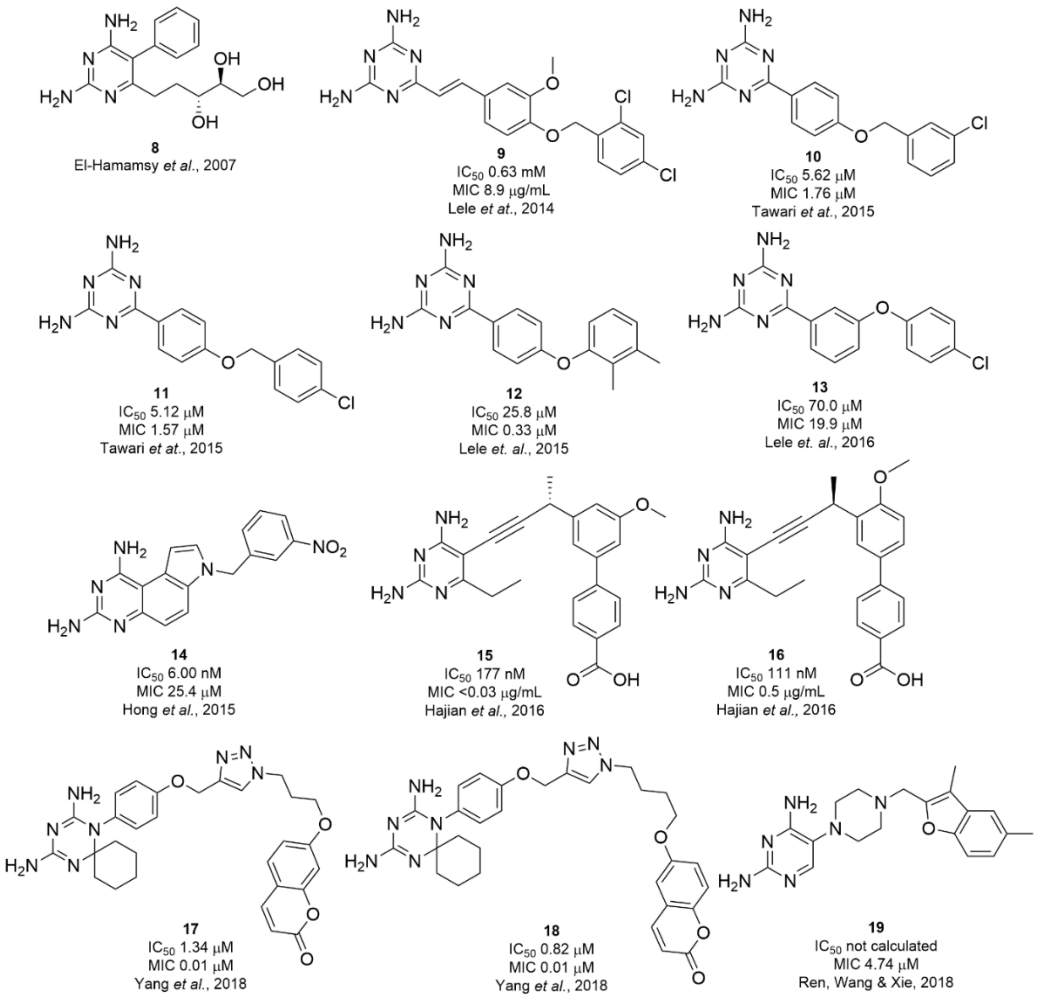

Figure 4. Chemical structures of *Mt*DHFR inhibitors based in diamino heterocyclic rings.

In the following year, Tawari *et al.* [55] reported the synthesis of new derivatives of the diamino triazine ring, optimized by virtual screening and molecular docking, which indicated that compounds without the carbon linker had better interaction with the catalytic site of *Mt*DHFR. 26 compounds were synthesized and evaluated in enzymatic, cytotoxicity, and antimycobacterial assays.

Compounds 10 and 11 (Figure 4) showed promising results in the whole cell assay against H_{37}Rv strain with MIC of 1.76 and 1.57 μM, respectively, in addition to showing low cytotoxicity to VERO cells with CC_{50} >300 μM. In the enzymatic inhibition assay, compounds 10 and 11 showed IC_{50} of 5.6 μM and 5.2 μM against *Mt*DHFR, while for *h*DHFR the IC_{50} were 72.5 and 83.3 μM, respectively and, therefore, the selectivity index was 14.5 times higher for *Mt*DHFR [55]. The presence of the terminal benzylic ring appears to be essential for the activity of the compounds since the replacement of this group by a pentyl ring led to the loss of anti-TB activity. Contrary to what was observed in the previous work by Lele *et al.* [54], compounds disubstituted in the benzylic aromatic ring and the addition of a methoxyl group in the phenolic ring were not well tolerated and caused a decrease in mycobactericidal activity.

Desagi's group also published two more papers [56,57] exploring the best substituents for the phenolic ring in the *para* and *meta*-position to triazine ring. About 16 compounds were synthesized for each position, but only compounds 12 [56] and 13 [57] (Figure 4) showed satisfactory anti-TB activity for each series in the whole cell assay against H_{37}Rv strain with a MIC of 0.33 μM for 12 and 19.9 μM for 13. Regarding the enzyme assay, compound 12

presented IC_{50} of 25.9 μM for *Mt*DHFR, a result much higher than that presented by compound 13, in which IC_{50} was 70.0 μM.

These results indicate that the position of the phenolic ring plays a strong influence on both the antimycobacterial and the inhibitory activity of the *Mt*DHFR enzyme, and the replacement of the benzyl ring by the phenyl ring also negatively impacts the inhibitory activity, indicating that the use of spacers can be well tolerated.

Hong *et al*. [46], based on the GOL pocket and the MTX binding mode, created a pharmacophoric model, which was further used to select ligands by virtual screening. The chosen compounds were synthesized and evaluated in an *in vivo* inhibition assay against *Mtb* strains ($H_{37}Ra$) and enzymatic inhibition assay against *Mt*DHFR and *h*DHFR. Although 40 compounds were tested, only 8 molecules showed inhibitory activity against *Mt*DHFR, among these compound 14 (Figure 4) was more active. The second most selective, with IC_{50} values of 6.0 nM and 33 nM for *Mt*DHFR and hDHFR, respectively, it was also the most active in the antimycobacterial assay with a MIC of 25.4 μM [46].

Molecular docking was used to determine interactions between 14 and *Mt*DHFR enzymes. The analysis of possible binding poses showed that 14 occupies the same position as MTX at the binding site but without touching GOL binding pocket. Although the authors carried out experiments to simulate molecular dynamics between 14 and both DHFR *Mtb* and human, they were not able to identify specific interactions that justify the selectivity observed in the enzyme inhibition assay [46].

With the diaminopyrimidine-phenolic ring as the pharmacophore, Hajian *et al*. [58] proposed the synthesis of new *Mt*DHFR inhibitors with a propargyl linker between the diaminopyrimidine core and the phenolic ring. The prepared compounds were evaluated for their antimycobacterial activity against Erdmann *Mtb* strain and *Mt*DHFR inhibitory activity. Over the 22 compounds prepared, 9 showed anti-TB activity, highlighting compounds 15 and 16 (Figure 4) with MIC of <0.03 μg/mL and 0.5 μg/mL, respectively.

Compound 16 was the most active in the *Mt*DHFR enzyme inhibition assay with an IC_{50} of 111 nM, against 177 nM of 15, and both compounds showed more selectivity for the DHFR of *Mtb* than for humans with IC_{50} values of 1015 nM (15) and 1955 nM (16). The authors observed that the presence of the methyl group in propargyl promotes an increase in the inhibitory activity of *Mt*DHFR; however, the enantiomers configuration was not relevant to the activity. The inhibitory activity was also higher in compounds with the methoxyl substituent in the *ortho* position and the carboxylic acid group in the *para* position. The exchange of the terminal benzoic ring for the 4-pyridine ring, despite increasing the inhibitory activity on *Mt*DHFR, also caused a loss of selectivity and a decrease in the antimycobacterial action [58].

In previous work, Chui's group [59] reported that *N*-substituted 1,3,5-triazaspiro[5,5]-undeca-2,4-diene derivatives had low affinity for *h*DHFR also good antimicrobial activity. Aiming to obtain compounds with selective activity for *Mt*DHFR and anti-TB action, the triazaspiro moiety was functionalized in the saturated nitrogen with a phenyl, benzoyl, or coumarin ring through two types of connectors: a short one composed of an alkyl-triazole ring and a longer one with the addition of a phenolic ring. The aromatic groups were chosen to establish hydrophobic or/and hydrogen-bonding interactions [48].

Compounds 17 and 18 (Figure 4) were most active in the antimycobacterial assay against *Mtb* strain $H_{37}Rv$ and *M. bovis BCG* with the same MIC value of 0.01 μM and 0.02 μM, respectively. In the enzyme inhibition assay against *Mt*DHFR, the IC_{50} values obtained

were 1.34 μM (17) and 0.82 μM (18), while for *h*DHFR the IC_{50} values were 11.99 μM (17) and 15.32 μM (18) [48]. In the anti-TB assay with the *M.bovis BCG* strain, all compounds with the terminal phenyl and benzyl rings showed low or no activation. So, the authors postulated that the absence of the phenolic ring led to obtaining inactive compounds. On the other hand, the increase in the alkyl linker chain resulted in compound good inhibitory activity against *Mt*DHFR.

The interaction between compound 18 and *Mtb* and human DHFR by molecular docking demonstrated that the compound establishes more favorable hydrogen-bonding interactions with the *Mt*DHFR binding site over *h*DHFR. According to the authors, the selectivity of compound 18 is related to the cyclohexyl spiro ring, which blocks the entry of the inhibitor into the catalytic site of *h*DHFR by steric hindrance [48].

In 2018, Ren, Wang, and Xie [60], using machine learning techniques designed a pharmacophore model predicting the main *Mt*DHFR active site interactions and screened the ChemBridge database for compounds with potential inhibitory activity. From a total of 131 compounds selected and tested against the *M. smegmatis* strain, only 4 structures showed antimycobacterial activity, being later tested against *Mtb* strain H_{37}Rv and inhibitory activity against *Mtb* and human DHFR.

Among the tested compounds, 19 (Figure 4) showed the best result in the anti-TB assay with the MIC value of 4.74 μM. The enzyme inhibition assay was carried out with a fixed concentration (20 μg/mL), and 19 showed an inhibition activity rate of 85.3% for *Mt*DHFR and 74.5% for *h*DHFR [60].

2.3. Non-traditional core-base structures.

To evaluate unconventional pharmacophores as potential *Mt*DHFR inhibitors, Shelke *et al*. [61] reported the synthesis of a fragment library of nitrogen heterocycles derivatives, including cyanouracil, xanthines, and quinazolinones selected on a virtual screening campaign. Molecular docking studies indicated that all tested fragments interacted with the *Mt*DHFR active site. The docking simulations predicted hydrogen bond donors between heterocycle nitrogen and Ile94 residue, and several fragments also exhibited good interaction with Asp27. Xanthines (20-22) and quinazolin-4-one (23 and 24) fragments showed additional interaction by π-stacking with Phe31 [61]. Overall, 20 compounds were prepared, and all of them exhibited some level of inhibition against *Mt*DHFR with IC_{50} in the range of 38 and 90 μM and antimycobacterial activity against *Mtb* H_{37}Rv strain. Figure 5 shows the most promising inhibitory activity compounds based on this approach [61].

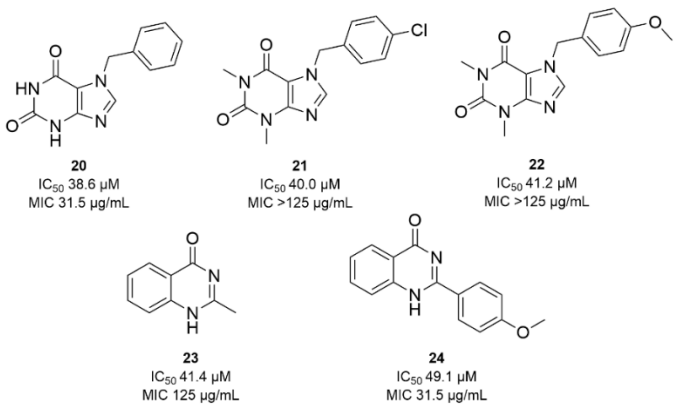

Figure 5. The chemical structure of the most activity compounds tested as a potential inhibitor of *Mt*DHFR (adapted from ref. 61).

Based on molecular docking and virtual screening studies, Sharma *et al*.[45] discovered a benzyl-indole ligand (Figure 6) as a potential inhibitor of *Mt*DHFR with possible points for substitution and improvement of the activity. From this, it was developed 11 inhibitors against *Mt*DHFR. Among them, compound 25 showed the best anti-TB action with MIC value of 25 μM, and it was the only one tested in the inhibitory enzymatic assay that showed IC_{50} of 150 μM and 980 μM for *Mt*DHFR and *h*DHFR, respectively.

Subsequent docking studies indicated that replacing the ketone group for amide group, carboxyl acid, propionamide, or diketoamide groups reduced the interaction with the binding site of *Mt*DHFR. Another unfavorable substitution is replacing the methyl group with any higher alkyl chain. And the benzyl ring interacts with residues of the GOL binding pocket, which corroborates the selectivity for *Mt*DHFR [45].

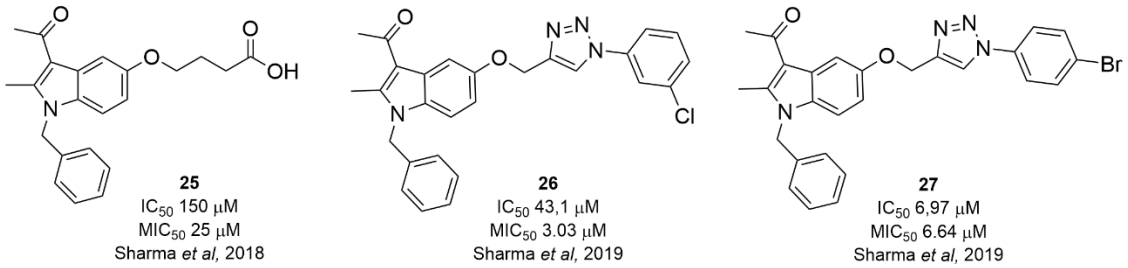

Figure 6. Chemical structures of benzyl-indole derivates designed as potential MtDHFR inhibitors.

Sharma *et al*. [62] also reported the optimization of compound 25 by replacing the carboxylic group with a substituted triazole ring that improved biological activity. Among the 20 synthesized compounds, 26 and 27 showed the most promising results with MIC_{50} values against *Mtb* $H_{37}Rv$ of 3.03 μM and 6.64 μM, respectively. *In vitro* enzymatic inhibition assay using *Mt*DHFR and *h*DHFR, the IC_{50} values were 43.1 μM (26) and 6.97 μM (27) for *Mt*DHFR and 180 μM (26), and 125 μM (27) for *h*DHFR, which indicated that these compounds were 20 to 80 times more selective than MTX (selectivity index of 4.17 for 27, 18.4 for 26 and 0.194 for MTX) [62].

Using docking studies, it was observed that the addition of the methylene triazole ring showed an improvement in the fit of the benzyl-indole derivatives with the *Mt*DHFR, increasing the inhibitory activity; on the other hand, the addition of electron-withdrawing substituents on the benzylic ring leads to a loss of activity, as well as substituents on the *ortho* position. It was observed that inhibitor 27 interacts with Gln28 and Phe31 from *Mt*DHFR. The authors suggest that this compound might reach the GOL binding pocket and consequently has higher selectivity for *Mt*DHFR [62]

Through a structure-based virtual screening strategy, Sharma *et al*. [63] tested the MolMall database seeking compounds with inhibitory activity against *Mt*DHFR. Based on docking score, binding interactions, and visual analysis 16 compounds were selected to be further evaluated for in vitro and enzymatic assays. Even though all compounds exhibited anti-TB activity against $H_{37}Rv$ strains, only compounds 28 and 29 (Figure 7A) showed MIC lower than 15 μM (0.65 μM and 12.5 μM respectively), and they were selected for enzymatic assay [63].

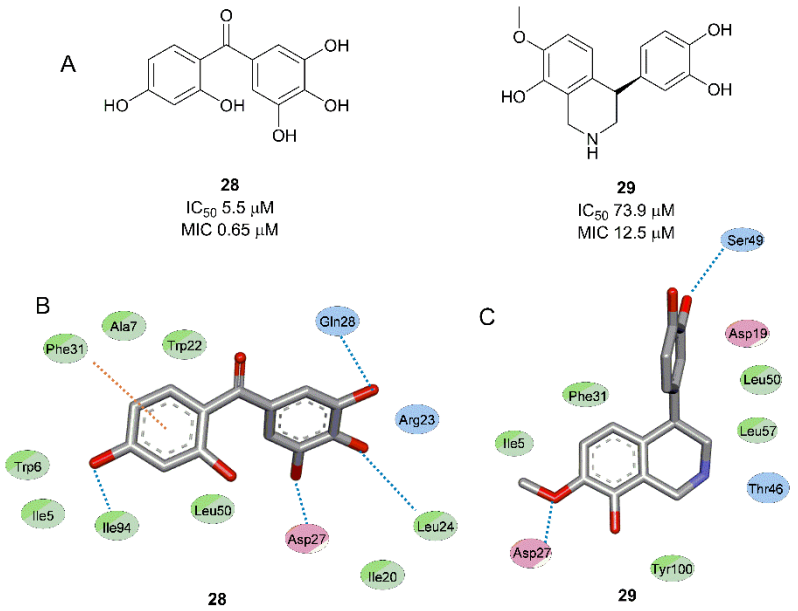

Figure 7. A) *Mt*DHFR inhibitors selected to *in vitro* and enzymatic studies after being identified by structure-based virtual screening; B) Main interactions of prototype inhibitor and *Mt*DHFR: orange dots: π-alkyl; blue dots: hydrogen bond (adapted from ref. 63). 3D images were drawn in Discovery Studio, Biovia.

Compounds 28 and 29 showed inhibitory activities against *Mt*DHFR with an IC_{50} 5.50 μM and 73.9 μM, respectively. In the enzymatic assay against *h*DHFR, an IC_{50} of 42 μM was obtained for 28 and 263 μM for 29, indicating that compound 28 has higher selectivity than 29, as predicted by the virtual screening simulations. The 2,4-dihydroxyphenyl group 28 was predicted by molecular docking to interact in the binding site of *Mt*DHFR by a hydrogen bond with the Ile94 residue and π-stacking with Phe31 (Figure 7B). In contrast, the hydroxyl groups from the 3,4,5-trihydroxyphenyl of 29 interact through hydrogen bonds with Gln28, Asp27 and Leu24 residues from GOL binding pocket (Figure 7C) [63].

The methoxy group of 29 interacts with Asp27 residue from GOL binding site as a hydrogen acceptor. Thus, it is possible to observe that the position of the functional groups of 29 caused a decrease in interaction with the enzyme, reflected by the higher IC_{50} value and less selectivity when compared to compound 28 [63].

Recently, Kronenberger *et al*. [64] also reported the design and synthesis of a substituted 3-benzoic acid derivative series as potential *Mt*DHFR inhibitors. The start point for this series was chosen among 17 fragments of hits previously identified by Ribeiro *et al*. [65]. Fragment 30 (Figure 8), despite having a low affinity against *Mt*DHFR (0.5 mM), has an on-target specific activity and a reasonable ligand efficiency (LE = 0.26). Altogether, 20 substituted 3-benzoic acid compounds were prepared, and three of them had an IC_{50} lower than 35 μM (31-33) and the most active compound 33 (IC_{50} 7.0 μM), is a classical bioisostere of 30 [64,65].

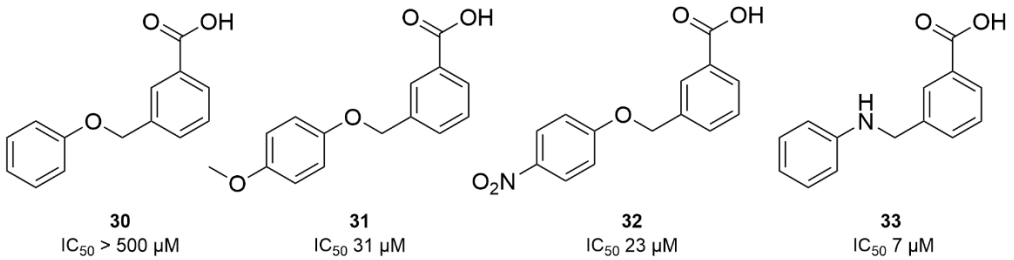

Figure 8. Chemical structure of substituted 3-benzoic acid derivative most promising results in the enzymatic inhibitory assay (adapted from ref. 64).

In the molecular dynamic simulation, Kronenberger *et al.* suggested that 33 has a temporary interaction with the Gln28, Ile20, and Ile94 residues. Compound 33 seems not to occupy the usual binding site of the enzyme; instead, it interacts with a unique pocket, composed of Arg32, Arg60, and occasionally, with Phe31. Therefore the data suggests that 33 has an uncompetitive inhibition mechanism, and it is stabilized by the closed-state *Mt*DHFR conformation [64].

2.4. Theoretical modeling of prototype inhibitor.

In 2010, Kumar, Vijayakrishnan, and Subba Rao [42], through molecular modeling studies, evaluated *in silico* the inhibitory activity against *Mt*DHFR of tripeptides. For the design of the small peptides, at least one aromatic amino acid (tyrosine or tryptophan) was used, and no amino acid with an alkyl side chain was chosen. Around 17 tripeptides were evaluated by molecular docking, and compound 34 (Figure 9A) had the higher binding affinity (K_D) value with 1.78 nM for *Mt*DHFR and 209 nM for *h*DHFR.

The results of the dynamic molecular simulation (Figure 9B) demonstrated that the hydroxyl of internal tyrosine of 34 interacts by a hydrogen bond with Ser49 residue; the same interaction also was observed between the carbonyl group and the Gln28 residue. The indole ring of tryptophan interacts by hydrogen bonding with the Asp27 residue and also establishes a van der Walls-type interaction with the Pro58 residue. And the terminal carboxylic acid makes hydrogen bonds with residues Arg32 and Arg60 [42].

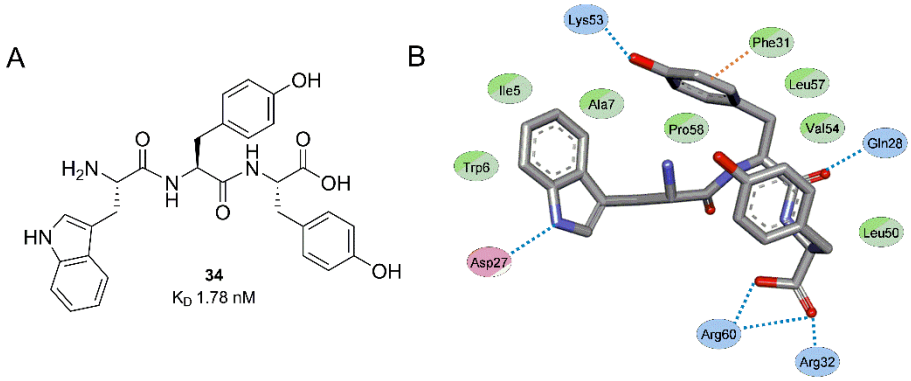

Figure 9. A) Chemical structure of tripeptide WYY; B) Main interactions of prototype inhibitor and *Mt*DHFR: orange dots: π-alkyl; blue dots: hydrogen bond (adapted from ref. 42). 3D images were drawn in Discovery Studio, Biovia.

2.5. Fragment-based discovery of prototype inhibitor.

Ribeiro *et. al.*[65] used several molecular biophysical techniques to identify low molecular weight compounds capable of binding in the unconventional active site of *Mt*DHFR. One of the aims of this study was to identify new scaffolds that could interact with the GOL-binding site, providing a starting point for more selective compounds. *Mt*DHFR-NADPH complex was screened against a library of fragments, in which compound 35 (Figure 10), a pyrazole *N*-aryl substituted, had K_D of 0.64 mM (LE = 0.28), and it binds to the GOL pocket of the enzyme and is selected to be optimized (36 and 37) [65].

The structural data of the *Mt*DHFR:NADPH complex and the compounds (35-37) indicates that adding a small alkyl linker attached to an indole ring increases the affinity of these compounds with the enzyme. The presence of a flexible linker allows the indole ring to reach different enzyme pockets; however, the aromatic ring always has a π-π interaction with

Phe31. The methyl group on the indole ring in 36 has a negative effect on the affinity, and a higher affinity of 37 could be associated with an additional interaction via hydrogen bonding between propanamide oxygen and the Gln28 side chain. Unfortunately, the structural modifications of fragment 35 caused the loss of interaction with the GOL pocket [65].

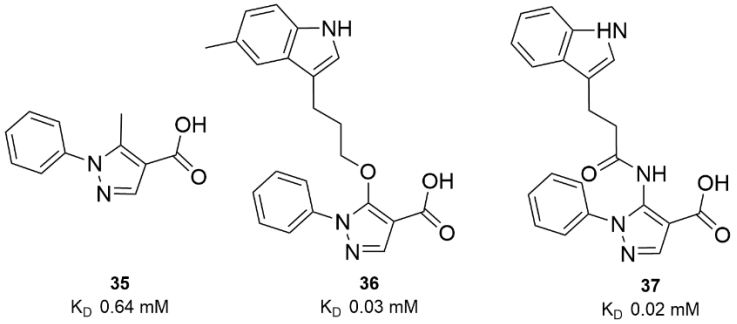

Figure 10. Chemical structure of pyrazole *N*-aryl derivatives (adapted from ref. 65).

2.6. Putative MtDHFR inhibitors.

Other derivatives of the 2,4-aminopyrimidine ring have also been used as a core base to obtain *Mt*DHFR inhibitors. Singh *et. al.*[66] in 2011 reported the design and prepared a series of hybrid molecules that could be used simultaneously as anti-tubercular and antidiabetic agents. The diabetic patient responds slowly to anti-TB treatment, and consequently, they are more susceptible to multidrug-resistant tuberculosis [67,68]. From previous independent work, these authors reported an anti-TB activity of a bis-benzylidene cycloalkanone derivative and the antidiabetic activity of the naphthyl-glycoside compound. To enhance the anti-TB activity, the bis-benzylidene cycloalkanones were functionalized with 2-aminopyrimidine. In a total, 20 compounds were prepared. Most of them exhibited moderate to good *in vitro* activity against $H_{37}Rv$ strains (MIC 6.25 µg/mL or 12.5 µg/mL), particularly the compound 38 (Figure 11), which showed a MIC of 3.12 µg/mL and a nontoxic activated against Vero cell line and mouse bone marrow-derived macrophages [66].

Although there is no description for the enzyme inhibition activity, 38 was predicted to be an effective ligand for *Mt*DHFR by molecular docking. The study indicated that 38 interacts with the enzyme in the *p*-aminobenzoic acid (PABA) binding site. The 2-aminopyrimidine nitrogen interacts by hydrogen bonds with Ile94 residue. In addition, a π-stacking interaction was also observed between Phe31 residue and one of 38 naphthalene rings; this interaction confers stability to the compound:enzyme complex facilitating catalytic activity. (Figure 11B). The *in-silico* simulation shows that 38 simultaneously occupy the NADPH and substrate binding sites. These interactions could explain this compound's high in vitro activity [66].

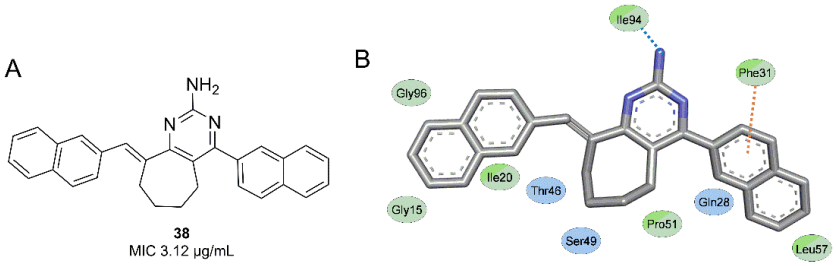

Figure 11. A) Chemical structure designed as dual function compound 38; B) Main interaction of inhibitor and *Mt*DHFR; orange dots: π-alkyl; blue dots: hydrogen bond (adapted from ref. 66). 3D images were drawn in Discovery Studio, Biovia

In 2016, Desai, Trivedi, and Khedkar [69] evaluated the anti-TB activity of new compounds prepared from the molecular hybridization of two different pharmacophores, with *Mt*DHFR as a molecular target. In the planned prototypes, the inhibitory action would be obtained using the dihydropyrimidinone ring as an analogous structure to 2,4-diaminopyrimidine, while the imidazole ring would be associated with antibacterial action.

From 16 compounds synthesized, three molecules (39-41) (Figure 12A) exhibited 97–99% *in vivo* inhibition against *Mtb* (H_{37}Rv strain) and had a MIC of 0.39, 0.78, and 0.39 µg/mL, respectively. These three compounds have electron-withdrawing substituents in the *para* position of the aromatic ring, which help increase the lipophilicity and favor the diffusion of the compounds through the cell membrane, facilitating the arrival of the molecules to the target [69].

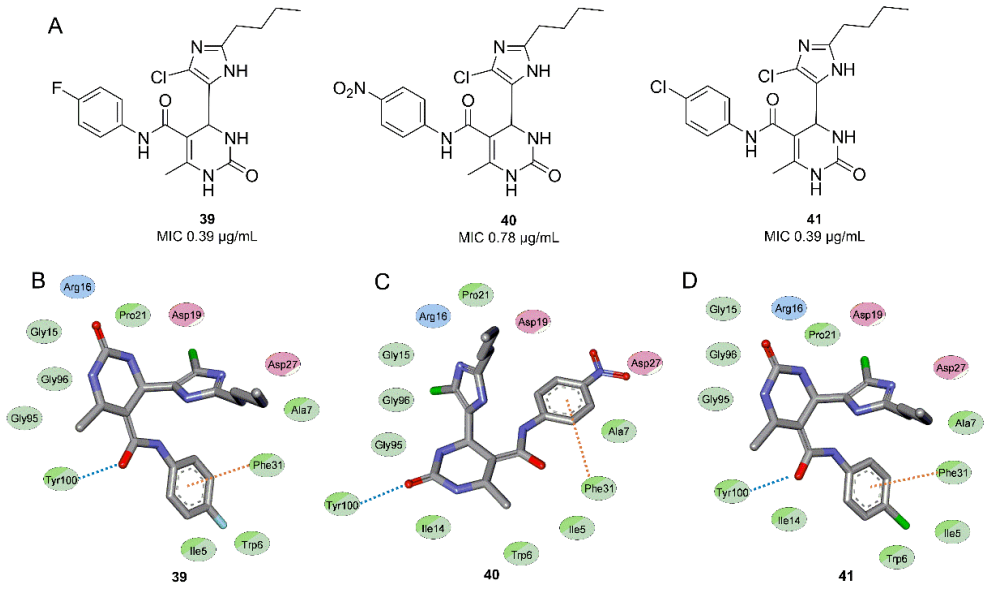

Figure 12. A) Chemical structure of anti-tubercular compounds proposed as potential inhibitors of *Mt*DHFR; B) Main interaction of inhibitor and *Mt*DHFR; orange dots: π-alkyl; blue dots: hydrogen bond (adapted from ref. 69). 3D images were drawn in Discovery Studio, Biovia.

Molecular docking simulations were used to investigate the potential inhibitory activity of the prepared compounds (39-41) over *Mt*DHFR. The results indicated that the imidazolyl 3,4-dihydro-pyrimidine-5-carboxamide moiety is stabilized by an extensive network in the binding site and also for van der Waals interactions. In addition, Desai, Trivedi, and Khedkar observed a favorable electrostatic interaction between these compounds with key residues involved in enzymatic activity. Besides that, compounds 39 and 40 interact through the hydrogen bond of the carboxamide oxygen atom and the hydroxyl group of the Tyr100 side chain. On the other hand, 41 was predicted to perform a hydrogen bond with the Tyr100 side chain through the oxygen atom of the pyrimidine ring. Furthermore, all compounds perform a π-stacking interaction between the substituted aromatic ring with Phe31 (Figure 12B-D) [69].

Liu et al. [70] screened compounds commercially to investigate new therapeutic targets for existing drugs, seeking antimycobacterial activity. Ceritinib 42 (Figure 13A), an antineoplastic drug with a 2,4 diamine-pyrimidine ring core, was identified as a potential anti-TB drug. The activity of 42 was verified by an *in vitro* assay against *Mtb* (H_{37}Ra strain), and the data showed that it had a moderate efficacy with a MIC of 9.0 µM. Inspired by the structure of 42, Liu *et al.* designed and synthesized 32 derivatives and evaluated their activity by *in vitro* assay against *Mtb* H37Ra strain.

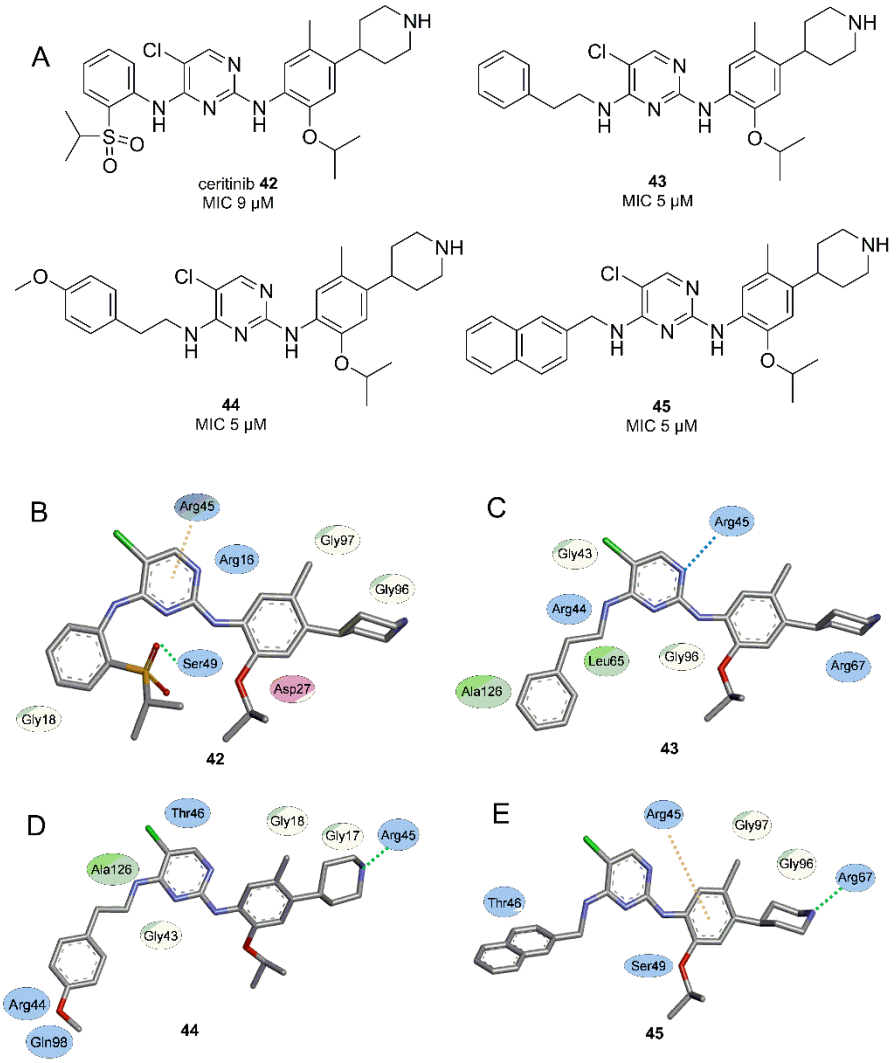

Figure 13. A) Chemical structure of ceritinib 42 and derivates (43-45) synthesized as potential inhibitors of *Mt*DHFR. Main interactions of prepared compounds and *Mt*DHFR: B) ceritinib (38); C) 39; D) 40; E) 41. Interaction: orange dots: π-alkyl; blue dots: hydrogen bond; green dots: π-sigma (adapted from ref. 70). 3D images were drawn in Discovery Studio, Biovia.

Three compounds bearing a 2-isopropoxy-5-methyl-4-(piperidin-4-yl)aniline group at position 2 and variable arylalkyl groups at position 4 of the pyrimidine ring (43-45) were the most active compounds with a MIC of about 5.0 µM. The anti-Tb activity observed for the prepared compounds was attributed to possible inhibitory action in *Mt*DHFR, since ceritinib and its derivatives have the pyridimine ring, which is the structural core related to the pharmacophore of DHFR inhibitors. *In silico* techniques were used to evaluate if the prepared compounds (42-45) showed interaction with *Mt*DHFR, thus justifying the anti-Tb activity observed by this mechanism of action [70].

Molecular docking simulations suggest that 42-45 interact with *Mt*DHFR but not in the same spot on the active binding site. The authors suggest that residue Arg45 has a key role in the interaction of 42-45. 42 pyrimidine ring forms a π-alkyl interaction with Arg45 (Figure 13B) while 43 nitrogen piperidine ring interacts through a hydrogen bond with Arg45 (Figure 13C). In compound 44 the nitrogen of the piperidine ring interacts with Arg45 by π-sigma bonds (Figure 13D), and in 45, the phenol ring also forms with Arg45 a π-alkyl interaction (Figure 13E) [70].

3. Conclusions and Perspectives

The participation of *Mt*DHFR in an important regulatory pathway for cell replication makes the inhibition of the catalytic activity of this enzyme a potential target for the development of anti-TB drugs. Initially, compounds derived or analogous to known antifolates, mainly MTX, were extensively developed and tested, and, with the aid of *in silico* techniques, the main binding sites were elucidated. The larger understanding of the structure-activity relationship between prototypes:enzyme allowed the development of compounds with structural core different from the traditional diaminopyrimidine, which enabled the observation of secondary binding sites.

However, the molecules with the most promising inhibitory activity are still those that have a nitrogen heterocycle as core-base, especially the diaminopyridine ring, which indicates that hydrogen bond-type interactions are very relevant for inhibitory activity. On the other hand, the search for more active compounds needs to be accompanied by structures capable of selectively interacting with the DHFR enzyme from *Mtb*. The mapping of key residues for catalytic activity and the difference in the size of the enzyme-binding cavity serves as a guide for exploring structures that have preferential fit to *Mt*DHFR. In addition, the *Mtb* enzyme features a unique hydrophilic pocket (GOL), which results in a key region for compound design with selectivity. The rational development of new inhibitors requires, therefore, obtaining compounds that can simulate the interactions observed by the pteridine ring, accessing key residues for catalytic activity in *Mt*DHFR, such as Arg32 and Arg60, for example, while being able to establish hydrophilic interactions with the GOL binding site, which could result in compounds with desirable pharmacological activity.

Although currently there is no compound in an advanced stage of a clinical study, *Mt*DHFR inhibitors still have great potential to be explored as a molecular target, not only because it plays a central role in the maintenance of the *Mtb* cell replication cycle, but also because of the vast structural knowledge of DHFR and its catalytic activity.

Funding

This research was supported by Coordenação de Aperfeiçoamento de Pessoal de Nível Superior—CAPES/Brazil (Finance Code 001). The authors are also grateful to Fundação de Amparo à Pesquisa do Estado de São Paulo—FAPESP/Brazil (grant no. 2013/18160-4 and 2017/00689-0).

Acknowledgments

We kindly acknowledge the grants supported by CAPES, CNPq, and FAPESP. V.B.N. also acknowledges CAPES for master fellowship.
All authors have read and agreed to the published version of the manuscript.

Conflicts of Interest

The authors declare no conflict of interest.

References

1. Quaglio, G.; Pizzol, D.; Bortolani, A.; Manenti, F.; Isaakidis, P.; Putoto, G.; Olliaro, P.L. Breast Tuberculosis in Women: A Systematic Review. *PLoS One* **2018**, *4*, 1–11, https://doi.org/10.4269/ajtmh.19-0061.

2. Patil, K.; Bagade, S.; Bonde, S.; Sharma, S.; Saraogi, G. Recent Therapeutic Approaches for the Management of Tuberculosis: Challenges and Opportunities. *Biomed. Pharmacother.* **2018**, *99*, 735–745, https://doi.org/10.1016/j.biopha.2018.01.115.
3. Garrido-Cardenas, J.A.; de Lamo-Sevilla, C.; Cabezas-Fernández, M.T.; Manzano-Agugliaro, F.; Martínez-Lirola, M. Global Tuberculosis Research and Its Future Prospects. *Tuberculosis* **2020**, *121*, 101917–101923, https://doi.org/10.1016/j.tube.2020.101917.
4. Colangeli, R.; Gupta, A.; Vinhas, S.A.; Chippada Venkata, U.D.; Kim, S.; Grady, C.; Jones-López, E.C.; Soteropoulos, P.; Palaci, M.; Marques-Rodrigues, P.; Salgame, P.; Ellner, J.J.; Dietze, R.; Alland, D. Mycobacterium tuberculosis progresses through two phases of latent infection in humans. *Nature Communications* **2020**, *11*, 1–10, https://doi.org/10.1038/s41467-020-18699-9.
5. Seifert, M.; Vargas, E.; Ruiz-Valdepeñas Montiel, V.; Wang, J.; Rodwell, T.C.; Catanzaro, A. Detection and Quantification of Mycobacterium Tuberculosis Antigen CFP10 in Serum and Urine for the Rapid Diagnosis of Active Tuberculosis Disease. *Sci. Rep.* **2021**, *11*, 19193–19203, https://doi.org/10.1038/s41598-021-98471-1.
6. Sun, L.; Chen, Y.; Yi, P.; Yang, L.; Yan, Y.; Zhang, K.; Zeng, Q.; Guo, A. Serological Detection of Mycobacterium Tuberculosis Complex Infection in Multiple Hosts by One Universal ELISA. *PLoS One* **2021**, *16*, 0257920–0257938, https://doi.org/10.1371/journal.pone.0257920.
7. *WHO | Global Tuberculosis Report 2020*. World Health Organization, Volume 5, **2020.**
8. Eshetie, S.; Gizachew, M.; Alebel, A.; Van Soolingen, D. Tuberculosis Treatment Outcomes in Ethiopia from 2003 to 2016, and Impact of HIV Co-Infection and Prior Drug Exposure: A Systematic Review and Meta-Analysis. *PLoS One* **2018**, *13*, 1–18, https://doi.org/10.1371/journal.pone.0194675.
9. Kritski, A.; Andrade, K.B.; Galliez, R.M.; Maciel, E.L.N.; Cordeiro-Santos, M.; Miranda, S.S.; Villa, T.S.; Ruffino Netto, A.; Arakaki-Sanchéz, D.; Croda, J. Tuberculosis: Renewed Challenge in Brazil. *Rev. Soc. Bras. Med. Trop.* **2018**, *51*, 2–6, https://doi.org/10.1590/0037-8682-0349-2017.
10. Ismail, M.B.; Rafei, R.; Dabboussi, F.; Hamze, M. Tuberculosis, War, and Refugees: Spotlight on the Syrian Humanitarian Crisis. *PLoS Pathog.* **2018**, *6*, 1–6, https://doi.org/10.1371/journal.ppat.1007014.
11. Chernyaeva, E.; Rotkevich, M.; Krasheninnikova, K.; Lapidus, A.; Polev, D.E.; Solovieva, N.; Zhuravlev, V.; Yablonsky, P.; O'Brien, S.J. Genomic Variations in Drug Resistant Mycobacterium Tuberculosis Strains Collected from Patients with Different Localization of Infection. *Antibiotics* **2020**, *10*, 27–39, https://doi.org/10.3390/antibiotics10010027.
12. Sultana, Z.Z.; Hoque, F.U.; Beyene, J.; Akhlak-Ul-Islam, M.; Khan, M.H.R.; Ahmed, S.; Hawlader, D.H.; Hossain, A. HIV Infection and Multidrug Resistant Tuberculosis: A Systematic Review and Meta-Analysis. *BMC Infect. Dis.* **2021**, *21*, 51–64, https://doi.org/10.1186/s12879-020-05749-2.
13. Arora, G.; Bothra, A.; Prosser, G.; Arora, K.; Sajid, A. Role of Post-translational Modifications in the Acquisition of Drug Resistance in *Mycobacterium Tuberculosis*. *FEBS J.* **2021**, *288*, 3375–3393, https://doi.org/10.1111/febs.15582.
14. Pires, G. M.; Do, M.; Martins, R. O.; Chicumbe, S.; Fronteira, I. Assessment of Directly Observed Therapy for Tuberculosis-A Systematic Literature Review. *ECronicon Pulmonol. Respir. Med.* **2018**, *7*, 669–680.
15. Palucci, I.; Delogu, G. Host Directed Therapies for Tuberculosis: Futures Strategies for an Ancient Disease. *Chemotherapy* **2018**, *63*, 172–180, https://doi.org/10.1159/000490478.
16. Drusano, G.L.; Neely, M.N.; Kim, S.; Yamada, W.M.; Schmidt, S.; Duncanson, B.; Nole, J.; Mtchedlidze, N.; Peloquin, C.A.; Louie, A. Building Optimal Three-Drug Combination Chemotherapy Regimens. *Antimicrob. Agents Chemother.* **2020**, *64*, 1–13, https://doi.org/10.1128/AAC.01610-20.
17. Sarinoglu, R.C.; Sili, U.; Eryuksel, E.; Yildizeli, S.O.; Cimsit, C.; Yagci, A.K. Tuberculosis and COVID-19: An Overlapping Situation during Pandemic. *J. Infect. Dev. Ctries.* **2020**, *14*, 721–725, https://doi.org/10.3855/jidc.13152.
18. Sheikh, B.A.; Bhat, B.A.; Mehraj, U.; Mir, W.; Hamadani, S.; Mir, M.A. Development of New Therapeutics to Meet the Current Challenge of Drug Resistant Tuberculosis. *Curr. Pharm. Biotechnol.* **2021**, *22*, 480–500, https://doi.org/10.2174/1389201021666200628021702.
19. Tiberi, S.; Scardigli, A.; Centis, R.; D'Ambrosio, L.; Muñoz-Torrico, M.; Salazar-Lezama, M.Á.; Spanevello, A.; Visca, D.; Zumla, A.; Migliori, G.B.; Caminero Luna, J.A. Classifying new anti-tuberculosis drugs: rationale and future perspectives. *International Journal of Infectious Diseases* **2017**, *56*, 181-184, https://doi.org/10.1016/j.ijid.2016.10.026.
20. Tiberi, S.; Pontali, E.; Tadolini, M.; D'Ambrosio, L.; Migliori, G.B. Challenging MDR-TB Clinical Problems – The Case for a New Global TB Consilium Supporting the Compassionate Use of New Anti-TB Drugs. *Int. J. Infect. Dis.* **2019**, *80*, S68–S72, https://doi.org/10.1016/j.ijid.2019.01.040.
21. Tweed, C.D.; Dawson, R.; Burger, D.A.; Conradie, A.; Crook, A.M.; Mendel, C.M.; Conradie, F.; Diacon, A.H.; Ntinginya, N.E.; Everitt, D.E.; Haraka, F.; Li, M.; van Niekerk, C.H.; Okwera, A.; Rassool, M.S.; Reither, K.; Sebe, M.A.; Staples, S.; Variava, E.; Spigelman, M. Bedaquiline, moxifloxacin, pretomanid, and pyrazinamide during the first 8 weeks of treatment of patients with drug-susceptible or drug-resistant pulmonary tuberculosis: a multicentre, open-label, partially randomised, phase 2b trial. *The Lancet Respiratory Medicine* **2019**, *7*, 1048-1058, https://doi.org/10.1016/S2213-2600(19)30366-2.

22. Palomino, C.J.; Ramos, F.D.; da Silva, A.P. New Anti-Tuberculosis Drugs: Strategies, Sources and New Molecules. *Current Medicinal Chemistry* **2009**, *16*, 1898-1904, https://doi.org/10.2174/092986709788186066.
23. Segretti, N.D.; Simões, C.K.; Corrêa, M.F.; Felli, V.M.A.; Miyata, M.; Cho, S.H.; Franzblau, S.G.; Fernandes, J.P.D.S. Antimycobacterial Activity of Pyrazinoate Prodrugs in Replicating and Non-Replicating Mycobacterium Tuberculosis. *Tuberculosis* **2016**, *99*, 11–16, https://doi.org/10.1016/j.tube.2016.04.002.
24. Raviglione, M.C.; Smith, I.M. XDR Tuberculosis - Implications for Global Public Health. *N. Engl. J. Med.* **2007**, *356*, 656–659, https://doi.org/10.1056/NEJMp068273.
25. García, J.I.; Allué-Guardia, A.; Tampi, R.P.; Restrepo, B.I.; Torrelles, J.B. New Developments and Insights in the Improvement of Mycobacterium Tuberculosis Vaccines and Diagnostics Within the End TB Strategy. *Curr. Epidemiol. Reports* **2021**, *8*, 33–45, https://doi.org/10.1007/s40471-021-00269-2.
26. Addla, D.; Jallapally, A.; Gurram, D.; Yogeeswari, P.; Sriram, D.; Kantevari, S. Rational Design, Synthesis and Antitubercular Evaluation of Novel 2-(Trifluoromethyl)Phenothiazine-[1,2,3]Triazole Hybrids. *Bioorganic Med. Chem. Lett.* **2014**, *24*, 233–236, https://doi.org/10.1016/j.bmcl.2013.11.031.
27. Dartois, V.; Barry, C.E. A Medicinal Chemists' Guide to the Unique Difficulties of Lead Optimization for Tuberculosis. *Bioorganic Med. Chem. Lett.* **2013**, *23*, 4741–4750, https://doi.org/10.1016/j.bmcl.2013.07.006.
28. Karoli, T.; Becker, B.; Zuegg, J.; Möllmann, U.; Ramu, S.; Huang, J.X.; Cooper, M.A. Identification of Antitubercular Benzothiazinone Compounds by Ligand-Based Design. *J. Med. Chem.* **2012**, *55*, 7940–7944, https://doi.org/10.1021/jm3008882.
29. Silva, R.E. da; Amato, A.A.; Guilhem, D.B.; de Carvalho, M.R.; Novaes, M.R.C.G. International Clinical Trials in Latin American and Caribbean Countries: Research and Development to Meet Local Health Needs. *Front. Pharmacol.* **2018**, *8*, 1–8, https://doi.org/10.3389/fphar.2017.00961.
30. Khawbung, J.L.; Nath, D.; Chakraborty, S. Drug resistant Tuberculosis: A review. *Comparative Immunology, Microbiology and Infectious Diseases* **2021**, *74*, 101574–101583, https://doi.org/10.1016/j.cimid.2020.101574.
31. Rivers, E.C.; Mancera, R.L. New anti-tuberculosis drugs in clinical trials with novel mechanisms of action. *Drug Discovery Today* **2008**, *13*, 1090-1098, https://doi.org/10.1016/j.drudis.2008.09.004.
32. Islam, M.M.; Hameed, H.M.A.; Mugweru, J.; Chhotaray, C.; Wang, C.; Tan, Y.; Liu, J.; Li, X.; Tan, S.; Ojima, I.; Yew, W.W.; Nuermberger, E.; Lamichhane, G.; Zhang, T. Drug resistance mechanisms and novel drug targets for tuberculosis therapy. *Journal of Genetics and Genomics* **2017**, *44*, 21-37, https://doi.org/10.1016/j.jgg.2016.10.002.
33. Evans, J.C.; Mizrahi, V. Priming the tuberculosis drug pipeline: new antimycobacterial targets and agents. *Current Opinion in Microbiology* **2018**, *45*, 39-46, https://doi.org/10.1016/j.mib.2018.02.006.
34. Silva, D.R.; Dalcolmo, M.; Tiberi, S.; Arbex, M.A.; Munoz-Torrico, M.; Duarte, R.; D'Ambrosio, L.; Visca, D.; Rendon, A.; Gaga, M. Novos fármacos e fármacos repropostos para o tratamento da tuberculose multirresistente e extensivamente resistente. *Jornal Brasileiro de Pneumologia* **2018**, *44*, 153-160.
35. Yang, R.; Tavares, M.T.; Teixeira, S.F.; Azevedo, R.A.; C. Pietro, D.; Fernandes, T.B.; Ferreira, A.K.; Trossini, G.H.G.; Barbuto, J.A.M.; Parise-Filho, R. Toward chelerythrine optimization: Analogues designed by molecular simplification exhibit selective growth inhibition in non-small-cell lung cancer cells. *Bioorganic & Medicinal Chemistry* **2016**, *24*, 4600-4610, https://doi.org/10.1016/j.bmc.2016.07.065.
36. DeJesus Michael, A.; Gerrick Elias, R.; Xu, W.; Park Sae, W.; Long Jarukit, E.; Boutte Cara, C.; Rubin Eric, J.; Schnappinger, D.; Ehrt, S.; Fortune Sarah, M.; Sassetti Christopher, M.; Ioerger Thomas, R.; Stallings Christina, L.; Manoil, C.; Lampe, D. Comprehensive Essentiality Analysis of the Mycobacterium Tuberculosis Genome via Saturating Transposon Mutagenesis. *MBio* **2017**, *8*, 1–17, https://doi.org/10.1128/mBio.02133-16.
37. Minato, Y.; Gohl, D.M.; Thiede, J.M.; Chacón, J.M.; Harcombe, W.R.; Maruyama, F.; Baughn, A.D. Genomewide Assessment of Mycobacterium Tuberculosis Conditionally Essential Metabolic Pathways. *mSystems* **2019**, *4*, 1–13, https://doi.org/10.1128/msystems.00070-19.
38. Vannucchi, H.; Monteiro, T. H. Ácido Fólico. In *Funções Plenamente Reconhecidas de Nutrientes*; ILSI Brasil,; ILSI Brasil: São Paulo, **2010**; Volume 10, pp 1–24.
39. Chawla, P.; Teli, G.; Gill, R. K.; Narang, R. K. An Insight into Synthetic Strategies and Recent Developments of Dihydrofolate Reductase Inhibitors. *ChemistrySelect*, **2021**, *6* (43), 12101–12145. https://doi.org/10.1002/slct.202102555
40. Osborne, M.J.; Schnell, J.; Benkovic, S.J.; Dyson, H.J.; Wright, P.E. Backbone Dynamics in Dihydrofolate Reductase Complexes: Role of Loop Flexibility in the Catalytic Mechanism. *Biochemistry* **2001**, *40*, 9846–9859, https://doi.org/10.1021/bi010621k.
41. Mugumbate, G.; Abrahams, K.A.; Cox, J.A.G.; Papadatos, G.; van Westen, G.; Lelièvre, J.; Calus, S.T.; Loman, N.J.; Ballell, L.; Barros, D.; Overington, J.P.; Besra, G.S. Mycobacterial Dihydrofolate Reductase Inhibitors Identified Using Chemogenomic Methods and In Vitro Validation. *Plos One* **2015**, *10*, https://doi.org/10.1371/journal.pone.0121492.
42. Kumar, M.; Vijayakrishnan, R.; Subba Rao, G. In Silico Structure-Based Design of a Novel Class of Potent and Selective Small Peptide Inhibitor of Mycobacterium Tuberculosis Dihydrofolate Reductase, a Potential

Target for Anti-TB Drug Discovery. *Mol. Divers.* **2010**, *14*, 595–604, https://doi.org/10.1007/s11030-009-9172-6.
43. Li, R.; Sirawaraporn, R.; Chitnumsub, P.; Sirawaraporn, W.; Wooden, J.; Athappilly, F.; Turley, S.; Hol, W.G.J. Three-Dimensional Structure of M. Tuberculosis Dihydrofolate Reductase Reveals Opportunities for the Design of Novel Tuberculosis Drugs. *J. Mol. Biol.* **2000**, *295*, 307–323, https://doi.org/10.1006/jmbi.1999.3328.
44. Li, P.; Xu, J.C. Total Synthesis of Cyclosporin O Both in Solution and in the Solid Phase Using Novel Thiazolium-, Immonium-, and Pyridinium-Type Coupling Reagents: BEMT, BDMP, and BEP. *J. Org. Chem.* **2000**, *65*, 2951–2958, https://doi.org/10.1021/jo991687c.
45. Sharma, K.; Tanwar, O.; Sharma, S.; Ali, S.; Alam, M. M.; Zaman, M. S.; Akhter, M. Structural Comparison of Mtb-DHFR and h-DHFR for Design, Synthesis and Evaluation of Selective Non-Pteridine Analogues as Anti-tubercular Agents. *Bioorg. Chem.* **2018**, *80*, 319–333, https://doi.org/10.1016/j.bioorg.2018.04.022.
46. Hong, W.; Wang, Y.; Chang, Z.; Yang, Y.; Pu, J.; Sun, T.; Kaur, S.; Sacchettini, J.C.; Jung, H.; Lin Wong, W.; Fah Yap, L.; Fong Ngeow, Y.; Paterson, I.C.; Wang, H. The identification of novel Mycobacterium tuberculosis DHFR inhibitors and the investigation of their binding preferences by using molecular modelling. *Scientific Reports* **2015**, *5*, 1-14, https://doi.org/10.1038/srep15328.
47. Ouyang, Y.; Yang, H.; Zhang, P.; Wang, Y.; Kaur, S.; Zhu, X.; Wang, Z.; Sun, Y.; Hong, W.; Ngeow, Y.F.; Wang, H. Synthesis of 2,4-Diaminopyrimidine Core-Based Derivatives and Biological Evaluation of Their Anti-Tubercular Activities. *Molecules* **2017**, *22*, https://doi.org/10.3390/molecules22101592.
48. Yang, X.; Wedajo, W.; Yamada, Y.; Dahlroth, S.L.; Neo, J.J.L.; Dick, T.; Chui, W.K. 1,3,5-Triazaspiro[5.5]Undeca-2,4-Dienes as Selective Mycobacterium Tuberculosis Dihydrofolate Reductase Inhibitors with Potent Whole Cell Activity. *Eur. J. Med. Chem.* **2018**, *144*, 262–276, https://doi.org/10.1016/j.ejmech.2017.12.017.
49. Dias, M.V.B.; Tyrakis, P.; Domingues, R.R.; Leme, A.F.P.; Blundell, T.L. Mycobacterium Tuberculosis Dihydrofolate Reductase Reveals Two Conformational States and a Possible Low Affinity Mechanism to Antifolate Drugs. *Structure* **2014**, *22*, 94–103, https://doi.org/10.1016/j.str.2013.09.022.
50. da Cunha, E. F. F.; Ramalho, T. C.; Reynolds, R. C. Binding Mode Analysis of 2, 4-Diamino-5-Methyl-5-Deaza-6-Substituted Pteridines with Mycobacterium Tuberculosis and Human Dihydrofolate Reductases. *J. Biomol. Struct. Dyn.* **2008**, *25*, 377–385, https://doi.org/10.1080/07391102.2008.10507186.
51. Nixon, M.R.; Saionz, K.W.; Koo, M.S.; Szymonifka, M.J.; Jung, H.; Roberts, J.P.; Nandakumar, M.; Kumar, A.; Liao, R.; Rustad, T.; Sacchettini, J.C.; Rhee, K.Y.; Freundlich, J.S.; Sherman, D.R. Folate Pathway Disruption Leads to Critical Disruption of Methionine Derivatives in Mycobacterium Tuberculosis. *Chem. Biol.* **2014**, *21*, 819–830, https://doi.org/10.1016/j.chembiol.2014.04.009.
52. Kumar, A.; Guardia, A.; Colmenarejo, G.; Pérez, E.; Gonzalez, R.R.; Torres, P.; Calvo, D.; Gómez, R.M.; Ortega, F.; Jiménez, E.; Gabarro, R.C.; Rullás, J.; Ballell, L.; Sherman, D.R. A Focused Screen Identifies Antifolates with Activity on Mycobacterium tuberculosis. *ACS Infectious Diseases* **2015**, *1*, 604-614, https://doi.org/10.1021/acsinfecdis.5b00063.
53. El-Hamamsy, M.H.R.I.; Smith, A.W.; Thompson, A.S.; Threadgill, M.D. Structure-based design, synthesis and preliminary evaluation of selective inhibitors of dihydrofolate reductase from Mycobacterium tuberculosis. *Bioorganic & Medicinal Chemistry* **2007**, *15*, 4552-4576, https://doi.org/10.1016/j.bmc.2007.04.011.
54. Arundhati, C.L.; Archana, R.; Ray, M.K.; Rajan, M.G.R.; Mariam, S.D. Design and Synthesis of Diaminotriazines as Anti-Tuberculosis DHFR Inhibitors. *Current Research in Drug Discovery* **2015**, *1*, 45–50, https://doi.org/10.3844/crddsp.2014.45.50.
55. Tawari, N.R.; Bag, S.; Raju, A.; Lele, A.C.; Bairwa, R.; Ray, M.; Rajan, M.G.R.; Nawale, L.U.; Sarkar, D.; Degani, M.S. Rational Drug Design, Synthesis and Biological Evaluation of Dihydrofolate Reductase Inhibitors as Antituberculosis Agents. *Future Med. Chem.* **2015**, *8*, 979–988, https://doi.org/10.4155/fmc.15.48.
56. Lele, A.C.; Raju, A.; Khambete, M.P.; Ray, M.K.; Rajan, M.G.R.; Arkile, M.A.; Jadhav, N.J.; Sarkar, D.; Degani, M.S. Design and Synthesis of a Focused Library of Diamino Triazines as Potential Mycobacterium Tuberculosis DHFR Inhibitors. *ACS Med. Chem. Lett.* **2015**, *6*, 1140–1144.
57. Lele, A.C.; Khambete, M.P.; Raju, A.; Ray, M.; Rajan, M.G.R.; Degani, M.S. Design and Synthesis of Novel Mycobacterium Tuberculosis DHFR Inhibitors. *Int. J. Pharm. Sci. Res.* **2016**, *7*, 2352–2356, https://doi.org/10.13040/IJPSR.0975-8232.7(6).2352-56.
58. Hajian, B.; Scocchera, E.; Keshipeddy, S.; Dayanandan, N.G.; Shoen, C.; Krucinska, J.; Reeve, S.; Cynamon, M.; Anderson, A.C.; Wright, D.L. Propargyl-Linked Antifolates Are Potent Inhibitors of Drug-Sensitive and Drug-Resistant Mycobacterium Tuberculosis. *PLoS One*, **2016**, *11*, https://doi.org/10.1371/journal.pone.0161740.
59. Ma, X.; Tan, S.T.; Khoo, C.L.; Sim, H.M.; Chan, L.W.; Chui, W.K. Synthesis and Antimicrobial Activity of N 1-Benzyl or N 1-Benzyloxy-1,6-Dihydro-1,3,5-Triazine-2,4-Diamines. *Bioorganic Med. Chem. Lett.* **2011**, *21*, 5428–5431, https://doi.org/10.1016/j.bmcl.2011.06.125.

60. Ren, J.X.; Wang, N.; Xie, Y. Identification of Novel DHFR Inhibitors for Treatment of Tuberculosis by Combining Virtual Screening with in Vitro Activity Assay. *J. Biomol. Struct. Dyn.* **2018**, *37*, 1054–1061, https://doi.org/10.1080/07391102.2018.1448721.
61. Shelke, R.U.; Degani, M.S.; Raju, A.; Ray, M.K.; Rajan, M.G.R. Fragment Discovery for the Design of Nitrogen Heterocycles as *Mycobacterium Tuberculosis* Dihydrofolate Reductase Inhibitors. *Arch. Pharm. (Weinheim).* **2016**, *349*, 602–613, https://doi.org/10.1002/ardp.201600066.
62. Sharma, K.; Tanwar, O.; Deora, G.S.; Ali, S.; Alam, M.M.; Zaman, M.S.; Krishna, V.S.; Sriram, D.; Akhter, M. Expansion of a Novel Lead Targeting M. Tuberculosis DHFR as Antitubercular Agents. *Bioorganic Med. Chem.* **2019**, *27*, 1421–1429, https://doi.org/10.1016/j.bmc.2019.02.053.
63. Sharma, K.; Neshat, N.; Sharma, S.; Giri, N.; Srivastava, A.; Almalki, F.; Saifullah, K.; Alam, M.M.; Shaquiquzzaman, M.; Akhter, M. Identification of Novel Selective *Mtb* -DHFR Inhibitors as Anti-tubercular Agents through Structure-based Computational Techniques. *Arch. Pharm. (Weinheim).* **2020**, *353*, https://doi.org/10.1002/ardp.201900287.
64. Kronenberger, T.; Ferreira, G.M.; de Souza, A.D.F.; da Silva Santos, S.; Poso, A.; Ribeiro, J.A.; Tavares, M.T.; Pavan, F.R.; Trossini, G.H.G.; Dias, M.V.B.; Parise-Filho, R. Design, synthesis and biological activity of novel substituted 3-benzoic acid derivatives as MtDHFR inhibitors. *Bioorganic & Medicinal Chemistry* **2020**, *28*, 115600–115610, https://doi.org/10.1016/j.bmc.2020.115600.
65. Ribeiro, J.A.; Hammer, A.; Libreros-Zúñiga, G.A.; Chavez-Pacheco, S.M.; Tyrakis, P.; de Oliveira, G.S.; Kirkman, T.; El Bakali, J.; Rocco, S.A.; Sforça, M.L.; Parise-Filho, R.; Coyne, A.G.; Blundell, T.L.; Abell, C.; Dias, M.V.B. Using a Fragment-Based Approach to Identify Alternative Chemical Scaffolds Targeting Dihydrofolate Reductase from Mycobacterium tuberculosis. *ACS Infectious Diseases* **2020**, *6*, 2192-2201, https://doi.org/10.1021/acsinfecdis.0c00263.
66. Singh, N.; Pandey, S.K.; Anand, N.; Dwivedi, R.; Singh, S.; Sinha, S.K.; Chaturvedi, V.; Jaiswal, N.; Srivastava, A.K.; Shah, P.; Siddiqui, M.I.; Tripathi, R.P. Synthesis, molecular modeling and bio-evaluation of cycloalkyl fused 2-aminopyrimidines as anti-tubercular and antidiabetic agents. *Bioorganic & Medicinal Chemistry Letters* **2011**, *21*, 4404-4408, https://doi.org/10.1016/j.bmcl.2011.06.040.
67. Girardi, E.; Sañé Schepisi, M.; Goletti, D.; Bates, M.; Mwaba, P.; Yeboah-Manu, D.; Ntoumi, F.; Palmieri, F.; Maeurer, M.; Zumla, A.; Ippolito, G. The global dynamics of diabetes and tuberculosis: the impact of migration and policy implications. *International Journal of Infectious Diseases* **2017**, *56*, 45-53, https://doi.org/10.1016/j.ijid.2017.01.018.
68. Liu, Q.; Li, W.; Xue, M.; Chen, Y.; Du, X.; Wang, C.; Han, L.; Tang, Y.; Feng, Y.; Tao, C.; He, J.-Q. Diabetes mellitus and the risk of multidrug resistant tuberculosis: a meta-analysis. *Scientific Reports* **2017**, *7*, 1090–1097. https://doi.org/10.1038/s41598-017-01213-5.
69. Desai, N.C.; Trivedi, A.R.; Khedkar, V.M. Preparation, biological evaluation and molecular docking study of imidazolyl dihydropyrimidines as potential Mycobacterium tuberculosis dihydrofolate reductase inhibitors. *Bioorganic & Medicinal Chemistry Letters* **2016**, *26*, 4030-4035, https://doi.org/10.1016/j.bmcl.2016.06.082.
70. Liu, P.; Yang, Y.; Tang, Y.; Yang, T.; Sang, Z.; Liu, Z.; Zhang, T.; Luo, Y. Design and Synthesis of Novel Pyrimidine Derivatives as Potent Anti-tubercular Agents. *Eur. J. Med. Chem.* **2019**, *163*, 169–182, https://doi.org/10.1016/j.ejmech.2018.11.054.